Analysis of box girder based on cross-sectional variations

Alex Kurniawandy[1*], *Rendy* Dafrianto[1], *Ismeddiyanto*[1], *Muhammad* Aminsyah[2], and *Rhoma* BH[3]

[1]Civil Engineering Department, Faculty of Engineering, Universitas Riau, Pekanbaru, Riau, Indonesia
[2]Civil Engineering Department, Faculty of Engineering, Universitas Andalas, Padang, West Sumatra, Indonesia
[3]Civil Engineering Department, Tokyo Metropolitan University, 1-1 Minami-Osawa, Hachioji-shi, Tokyo, Japan

Abstract. Box girders are widely utilized in prestressed concrete bridge construction due to their high torsional stiffness and cost-effectiveness. This study analyzes the structural capacity of a prestressed concrete box girder bridge planned to span the Siak River in Pekanbaru City, consisting of a 97.5 meters main span and two side spans of 58.5 meters each. The bridge is constructed using the balanced cantilever method, allowing for a variable-depth girder profile to optimize performance during the construction stage. Structural analysis was carried out in both transverse and longitudinal directions using the finite element method. The analysis results show that the maximum prestress loss reached 272.22 MPa, equivalent to 19.94% of the initial prestressing stress. Stress evaluations at transfer and service stages were within the allowable limits specified by RSNI-T12-2004. Maximum deflections observed in the side and main spans were 33.21 mm and 80.89 mm, respectively, remaining within serviceability limits. The calculated ultimate capacities for bending, torsion, and shear were 1.20×10^6 kN.m, 3.36×10^4 kN.m, and 4.70×10^4 kN.m, respectively. These results confirm that the designed box girder structure fulfills both strength and serviceability requirements in accordance with national bridge design standards.

1 Introduction

Prestressed concrete girder bridges are widely used worldwide due to their mature construction technology, economical cost, and low maintenance [1]. Prestressed concrete is a composite material that integrates high-strength concrete with high-tensile steel, where the tensile stress induced in the steel is counteracted by the concrete, resulting in compression in one of the concrete fibers. The advantages of prestressed concrete is its capacity to improve structural strength and durability through deflection control and increasing internal compression, which partially counteract the stresses generated by applied loads on the structural element [2]. In bridge construction, prestressed concrete is utilized as the primary material for girder fabrication due to its capability to accommodate the design of structural elements with relatively long spans.

Currently, various innovations in girder design have been developed, such as I-girders, box girders, T-girders, and others. Among these, box girders are the most commonly adopted type in long-span prestressed bridge construction. Box girders offer superior torsional rigidity, which makes them particularly suitable for curved bridge structures, where increasing curvature angles result in significant torsional demands [3]. Moreover, compared to I-girders, box girders tend to be more cost-effective and involve reduced construction volume [4]. In the design process, box girders are generally configured with a constant depth when employing the span-by-span construction method, whereas variable depth profiles can be adopted when utilizing the balanced cantilever method.

This study will analyze a bridge located in the city of Pekanbaru, which is planned to utilize a prestressed concrete box girder structure. The bridge consists of two side spans, each measuring 58.5 meters, and a main span measuring 97.5 meters. The bridge is constructed using the balanced cantilever method, chosen as an effective solution for long-span bridge construction—particularly for spanning the Siak River, which has an approximate width of 75 meters. This method eliminates the requirement for shoring, thereby reducing direct interaction with the underlying terrain.

Numerous studies on the capacity analysis of box girders have been conducted to investigate the internal forces and the resulting structural capacity. Trisnawardhana et al. [5] evaluated the design of the Longspan LRT Cililitan Bridge, with the evaluation covering aspects such as tendon quantity, prestress losses, and deflection. Ranje and Shah [6] studied a balanced cantilever box girder bridge with varying span lengths of 60 m, 70 m, and 80 m. Their study indicated that increasing the span length leads to higher bending moments, shear forces, and deflections in the box girder section.

Kosim and Supartono [7] examined the capacity of box girders in balanced cantilever bridges. The analysis results from their study included the quantity of tendons used and the corresponding stress levels during both the construction and post-construction stages. Another study conducted by Kalaiselvan [8] revealed that the maximum

* Corresponding author: alexkurniawandy@eng.unri.ac.id

bending moment in a box girder occurs at the girder segment located above the bridge pier. This moment arises during construction loading in bridges utilizing the balanced cantilever method. Based on these studies, it is evident that the maximum bending moment must be reduced by modifying the girder cross section. Therefore, this research aims to analyze the capacity of box girders with variations in cross-sectional area. The capacity of each girder section will be analyzed using finite element software.

2 Prestressed concrete

2.1 Fiber stress distribution

According to Lin and Burns [9], prestressed concrete is concrete in which there have been introduced internal stressed of such magnitude and distribution that the stresses resulting from given external loadings are counteracted to a desired degree. Concrete is inherently weak in tension but strong in compression. The low tensile capacity of concrete can be overcome through the use of prestressed concrete. In prestressed concrete, a pre-applied stress is introduced to the concrete fibers that are expected to undergo tension under service loads. This internal stress induces a compressive force in the opposite direction of the applied external loads. Such counteracting stress indirectly provides tensile capacity to the prestressed concrete element. The normal stress (f) resulting from the external bending moment (M), prestressing force (P), and tendon eccentricity (e) can be determined using the distribution expressed in Equation (1).

$$f=\frac{P}{A}\pm\frac{P.e.C}{I}\mp\frac{M.C}{I} \qquad (1)$$

Where, (A) is the cross-sectional area of the concrete, (C) is the distance from the extreme fiber to the centroid of the concrete section, and (I) represents the moment of inertia of the section.

2.2 Loss of prestressed

The progressive reduction of prestressing force in prestressed concrete elements is referred to as prestress loss. According to Nawy [10], prestress loss is caused by several factors that can be categorized into two main criteria, namely:

1. Immediate elastic losses, which occur during fabrication and construction processes, include elastic shortening of concrete, anchorage slip, and prestress loss due to friction.
2. Time-dependent losses refer to prestress losses that develop during service conditions, such as shrinkage, creep, temperature effects, and steel relaxation.

3 Case study

A prestressed box girder bridge is used as the case study in this research, in which its structural capacity will be investigated. The bridge is located in Pekanbaru City, Riau Province, crossing the Siak River, and consists of two side spans and one main span. Each side span measures 58.5 meters, while the main span measures 97.5 meters. The total width of the bridge is 16.3 meters, flanked by two barriers, each 0.5 meters wide. The superstructure of the bridge comprises several segments with varying heights, as illustrated in Fig. 1.

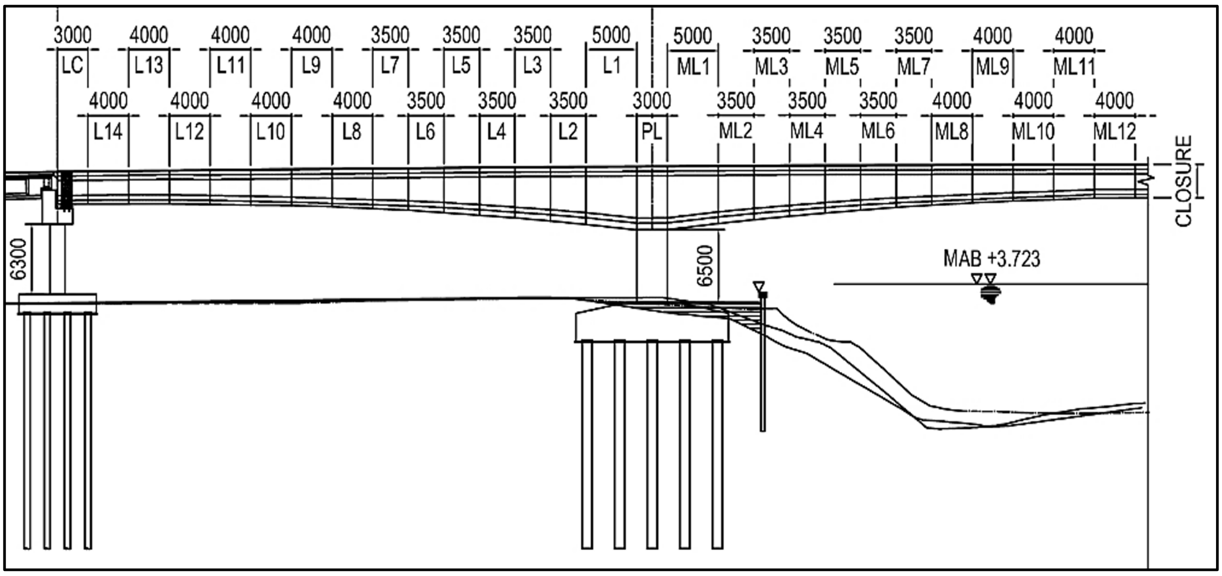

Fig. 1. Long section of prestressed box girder

The concrete used for the box girder has a specified compressive strength of 45 MPa. The reinforcement steel is of type BJTS 550, with a tensile strength of 687.5 MPa and a yield strength of 550 MPa. For the prestressing tendons, ASTM(S) standard A416-270 (Low) type strands are used. The strand diameter is 0.6 inches for longitudinal tendons and 0.5 inches for transverse tendons. The ultimate tensile strength of the strand (f_{pu}) is 1860 MPa, with a jacking stress of 1365 MPa (equivalent to 75% of f_{pu}).

The typical box girder at the support area is represented by segment ML1, while the typical box girder at the mid-span area is represented by segment ML12. The geometric details of the support box girder (ML1) and the mid-span box girder (ML12) are shown in Fig. 2 and Fig. 3, respectively.

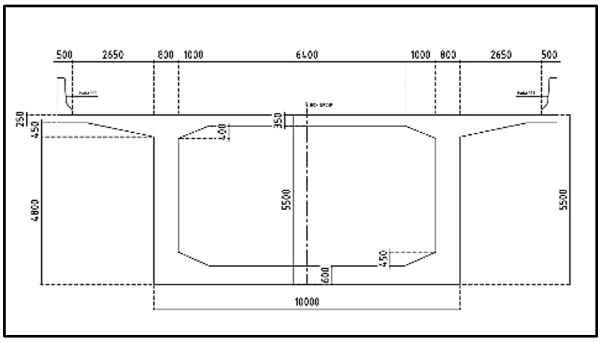

Fig. 2. Typical cross-section of the support box girder (ML1)

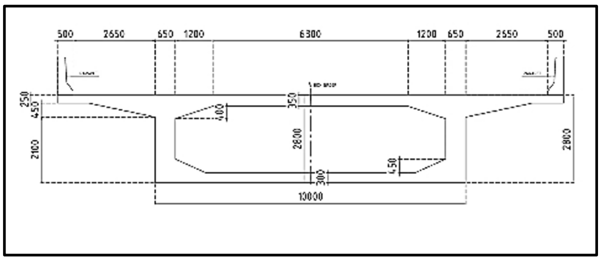

Fig. 3. Typical cross-section of the mid-span box girder (ML12)

4 Transverse analysis

The box girder possesses a distinctive characteristic in its top flange, which comprises the main top slab and cantilever (overhang) slab. Among various girder types, the box girder features the longest overhang span. In general, the length of the side cantilever of a conventional box girder is less than 4 m, and the transverse bending moment capacity is the controlling factor for the dimensions of the bridge deck [11]. The top slab of the box girder is also prestressed transversely. Transversely post-tensioned precast concrete deck unit is effective in providing load distribution between beams compared to 'traditional in-situ deck bridges [12]. Consequently, transverse analysis is essential to evaluate the distribution of moments acting in the lateral direction of the bridge. This analysis is necessary to represent the moment distribution resulting from both permanent and live loads in accordance with AASHTO LRFD specifications. The outcomes of this analysis serve as the basis for designing transverse reinforcement in the top slab, bottom slab, web, and cantilever slab regions [13].

In the transverse analysis process, an approximate method is employed as the structural analysis technique. The approximate method involves dividing the bridge structure into strips that represent the global structure in order to calculate the effects (internal forces and deformations) resulting from loads acting on the bridge. The dead load effects, consisting of moment and shear (MA and MS) on the slab, are calculated based on a slab strip width of 1000 mm. The dead loads acting on the slab include the self-weight of the slab, parapet loads, and the wearing surface (pavement) loads.

The live load effects (moment and shear) on the slab are determined using the equivalent strip width approach. The equivalent strip width varies depending on the type of slab, the direction of the principal strip being considered, and the slab location (cantilever zone, positive moment region, or negative moment region). The determination of the equivalent slab strip width (W) for the calculation of vehicular live load effects on cast-in-place concrete girder slabs can be conducted using Equation 2, Equation 3, and Equation 4, where X is the clear distance of the cantilever slab, and S is the clear spacing between the top slab and the cantilever slab.

$$W=1140+0,833X\ (Cantilever) \tag{2}$$
$$W=660+0,55S\ (Positive\ Moment) \tag{3}$$
$$W=1220+0,25S\ (Negative\ Moment) \tag{4}$$

The live load considered in the transverse analysis consists solely of the design truck load. The design truck comprises a semi-trailer vehicle and its associated axle weights. Each axle load is distributed into two equal uniform loads, representing the contact areas between the wheels and the deck surface. According to SNI 1725:2016, when using the strip method to analyze vehicular floor slabs and slabs spanning in the transverse direction perpendicular to the traffic flow, only a single axle of the design truck is considered for calculating the design shear force or bending moment. The number of design trucks included in the analysis corresponds to the number of design lanes. The clear width of the bridge is 15.3 meters without a median, indicating that the required number of design lanes is six. The placement of the design truck axles is arranged with a transverse spacing of 1 meter between adjacent axles.

The structural analysis of the box girder cross-section is conducted using the finite element method by modeling the slabs as one-dimensional beams supported by several supports in the transverse direction of the bridge, as illustrated in Fig. 4. Various boundary conditions are applied in the transverse analysis model. However, simplified assumptions tend to yield more reasonable results [14]. In this transverse modeling, the box girder cross-section is assumed to have simple supports located at the bottom ends of the webs. The modeled strip has a width of 4 meters for both the support and midspan segments, as shown in Fig. 5.

The calculated dead loads include the parapet load with a unit weight of 24 kN/m² and an asphalt layer with a thickness of 10 cm (comprising 5 cm of initial thickness plus an additional 5 cm resurfacing layer), with a unit weight of 22 kN/m². For live load effects from vehicular traffic, the truck load is applied as a moving load, with each wheel distributing a force of 112.5 kN.

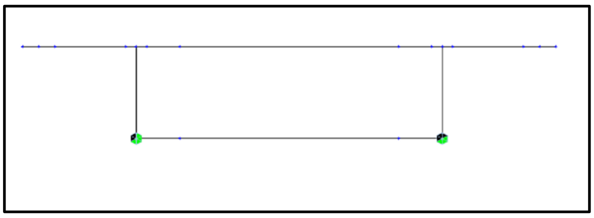

Fig. 4. Transverse modeling of box girder as a frame element

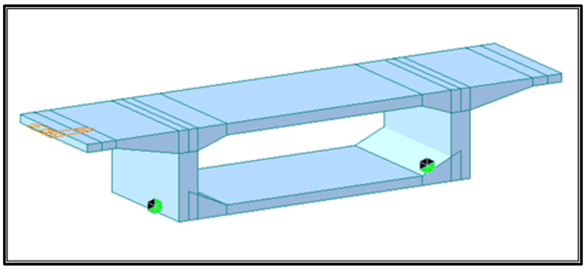

Fig. 5. Illustration of transverse modeling of box girder based on strip width

The transverse modeling of box girders based on a specified strip width needs to be adjusted to reflect the equivalent strip width influenced by live load effects. This adjustment can be performed by modifying the live load factor through scaling, using the ratio between the effective width and the modeled slab width. Table 1 and 2 present the modified live load factors resulting from the influence of the equivalent strip width.

Table 1. Modified load factors on support segment

Types of strip width	Clear distance between wings, X	Clear distance between top slab and wing slab, S	Strip width, be	Live load factor	
	mm	mm	mm	1	1.8
OH			3681	1.36	2.44
M+	3050	9200	5720	0.87	1.58
M-			3520	1.42	2.56

Table 2. Modified load factors on mid-span segment

Types of strip width	Clear distance between wings, X	Clear distance between top slab and wing slab, S	Strip width, be	Live load factor	
	(mm)	(mm)	(mm)	1	1.8
OH			3618	1.11	1.99
M+	2975	9350	5803	0.69	1.24
M-			3558	1.12	2.02

The results of the transverse analysis model, including the internal forces, are presented in Tables 3, 4 and 5. Each reinforced component of the box girder–namely the top slab, bottom slab, and web–requires different internal force values depending on the specific analytical process needed for each structural element.

Table 3. Internal forces in the top slab

Segment type	Bending Moment		Shear force	
	Support	Field	Support	Field
	kN.m	kN.m	kN	kN
ML1	2344.42	1003.5	1810.36	1271.10
ML2	1868.54	963.30	1473.44	1017.70

Table 4. Internal forces in the bottom slab

Segment type	Negative Moment	Positive Moment	Ultimate Shear	
			Support	Field
	kN.m	kN.m	kN	kN
ML1	1250.65	490.60	542.49	406.42
ML12	629.27	192.81	272.40	181.02

Table 5. Internal forces in the bottom slab

Segment type	Condition	P	Mx	My
		kN	kN.m	kN.m
ML1	Pu max.	-421.93	0	1661.97
	Pu min.	-3482.94	0	-1318.94
	My max.	-428.16	0	2179.72
	My min.	-2937.68	0	-2155.09
ML12	Pu max.	-312.65	0	1160.62
	Pu min.	-2539.37	0	-658.52
	My max.	-316.15	0	1788.13
	My min.	-2357.49	0	-1771.72

Based on the obtained internal forces, the transverse reinforcement can be determined by assuming that the slab components of the box girder behave as one-dimensional beam elements, while the web sections are analyzed using interaction diagrams. A summary of the box girder reinforcement is presented in Table 6.

Table 6. Recapitulation of transverse reinforcement

Components of box girder	Shear Zone	
	Support	Field
Top slab	D16-150	D16-150
Web	24D25	24D25
Bottom slab	D16-150	D16-150

5 Longitudinal analysis

5.1 Load

The loading configuration for the bridge is determined based on SNI 1725:2016. According to this standard, the bridge is analyzed under permanent loads (self-weight and superimposed dead loads), live loads (lane, truck, and braking forces), and additional static loads such as creep, shrinkage, prestressing, and temperature effects. Seismic loads are considered based on SNI 2833:2016. Structural performance is evaluated based on Ultimate Limit State (ULS) and Service Limit State (SLS) criteria.

5.2 Numerical model and structure analysis

The bridge was modeled using a three-dimensional finite element application to capture its structural behavior with adequate accuracy. In this model, the box girders and piers were idealized as line elements, allowing efficient representation of the global geometry, as illustrated in Fig. 6. All structural components were then assigned with appropriate boundary conditions and connectivity to form

https://doi.org/10.1051/e3sconf/202567706004

a complete analytical model. The finalized model, shown in Fig. 7, served as the basis for conducting the subsequent structural analysis.

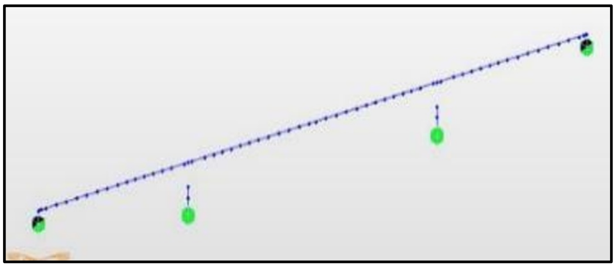

Fig. 6. Longitudinal modeling of balanced cantilever bridge as a line element

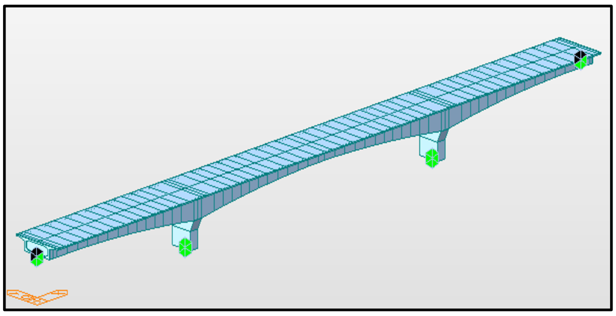

Fig. 7. Illustration of longitudinal modeling

Prestress losses are categorized into two types: immediate losses and time-dependent losses. Based on the prestress analysis, the greatest loss was observed in one of the bottom tendon profiles, with immediate losses amounting to 175.06 MPa and time-dependent losses of 82.96 MPa. Consequently, the total prestress loss for that tendon profile reached 272.22 MPa, which corresponds to 19.94% of the initial stress of 1365 MPa.

The longitudinal analysis considers two bridge conditions: during the construction stage and after the bridge has been completed. During the construction stage, the bridge structural system behaves as a cantilever. Construction stage analysis is essential to control the stresses that occur during this phase. The internal forces resulting from the construction stage analysis are illustrated in Figure 8. Any loads applied thereafter–such as superimposed loads including the asphaltic wearing surface and safety barriers, traffic loads, and other live loads–act on the completed bridge, which behaves as a continuous structural system [15]. Table 7 presents the internal forces acting after the bridge has been fully constructed. The resulting bending moment, torsional moment, and shear force serve as the basis for designing the longitudinal reinforcement.

Table 7. Recapitulation of internal forces

Internal Forces	Segment type	
	ML1	**ML12**
Bending moment (kN.m)	7347735.85	132175.25
Shear force (kN)	36096.64	15617.60
Torque moment (kN.m)	13240.00	12312.00

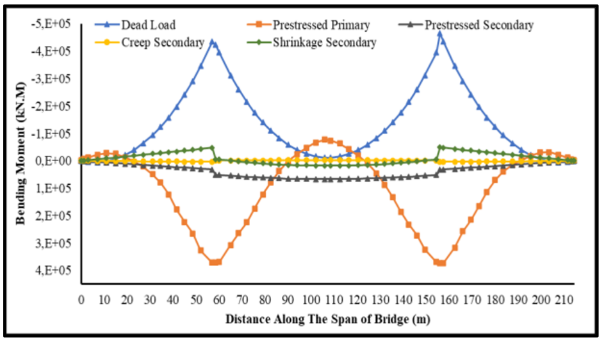

Fig. 8. Bending moment at construction stage

5.3 Stress and deflection limit

The compressive and tensile stress limits are regulated by RSNI-T12-2004 for both the immediate post-transfer stage and the service stage. At the time of prestress transfer, the age of the box girder segment is 7 days. Therefore, the compressive strength of prestressed concrete is reduced to 75%, resulting in a value of 33.75 MPa. The allowable tensile stress is 1.45 MPa, while the allowable compressive stress is 20.25 MPa. To calculate stresses immediately after prestress transfer, the dead loads for each construction stage must be considered. Fig. 9 and Fig. 10 show that the stresses during the construction stage remain within safe limits, with a compressive stress of 11.37 MPa and a tensile stress of 0.092 MPa.

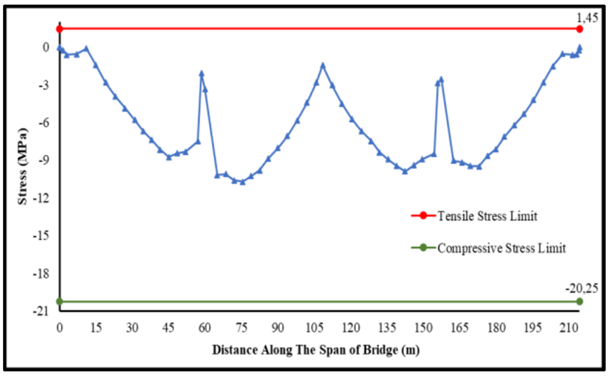

Fig. 9. stress diagram at the top fiber during the construction stage

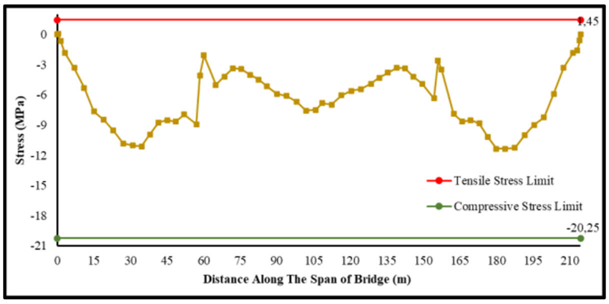

Fig. 10. Stress diagram at the bottom fiber during the construction stage

The service stage stress check refers to service load combinations. According to RSNI-T12-2004, the allowable tensile stress is 3.35 MPa, and the allowable compressive stress is 20.25 MPa. Based on Figs. 11 and

12, the stresses during the service stage–2.97 MPa in tension and 16.47 MPa in compression–are still considered safe and within the permissible stress limits for the service condition.

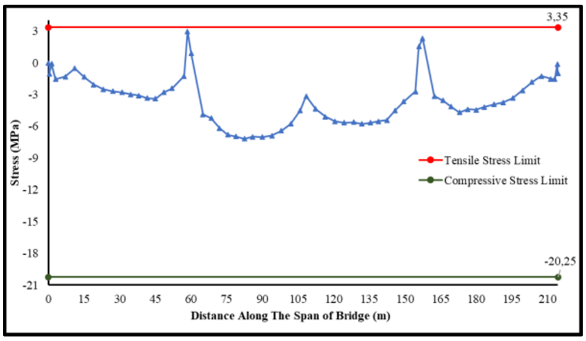

Fig. 11 Tensile stress check in service stage (Service load combination III)

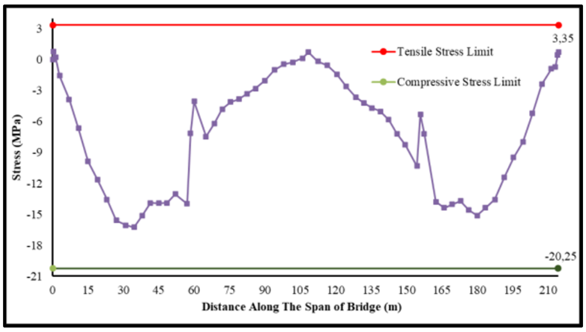

Fig. 12 Compressive stress check in service stage (Service load combination I)

Based on the structural analysis performed using finite element software, the deflection of the box girder cross-section can be determined. The deflection occurring in a box girder bridge must be limited under service conditions in accordance with RSNI-T12-2004, which specifies allowable deflection limits of *L/400* for cantilever structures and *L/800* for simply supported spans, where *L* represents the distance between inflection point. A point of inflection refers to the location along the span where the bending moment is zero on the moment diagram. The distance between points of contraflexure for the side span is 58.5 m, while for the main span it is 84.5 m. Therefore, the deflection limits are 146.25 mm for the side span and 105.63 mm for the main span.

Figure 13 illustrates the deflection occurring at each section of the box girder. In the side span, the maximum upward deflection is 33.21 mm, while in the main span, the maximum downward deflection is 80.89 mm. These results indicate that the deflections in both the side and main spans remain within the allowable deflection limits.

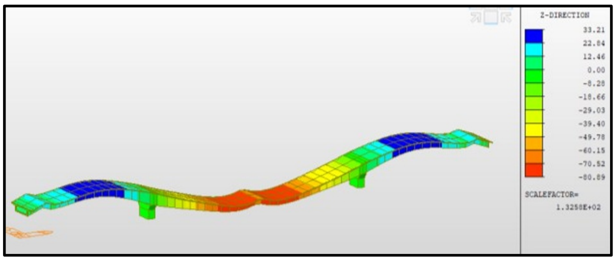

Fig. 13. Deflection in the box girder

5.4 Box Girder Capacity

Based on the internal forces obtained from the previous structural analysis, the longitudinal reinforcement of the box girder can be designed. The area of reinforcement provided is used to calculate the cross-sectional capacity by considering the combined contribution of both the concrete section and the prestressing tendons. The results of the reinforcement summary and the calculated sectional capacities are presented in Table 8 through Table 9.

Table 8. Summary of box girder capacity

Segment type	Flexural (kN.m)	Torsion (kN.m)	Shear (kN)
ML1	$1{,}20 \times 10^6$	$3{,}36 \times 10^4$	$4{,}70 \times 10^4$
ML12	$2{,}49 \times 10^5$	$1{,}77 \times 10^4$	$2{,}16 \times 10^4$

Table 9. Recapitulation of longitudinal reinforcement

Box girder component	Shear zone	
	Support	Field
Top slab	D16-150	D16-150
Web	D24-150	D24-150
Bottom slab	D16-150	D16-150

6 Conclusion

This study presents an analysis of the structural capacity of box girders with varying cross-sectional types. Based on the results of the structural modeling, analysis, and evaluation, the following conclusions can be drawn:

1) The highest internal forces occur in the support segment (ML1), including bending moment, torsional moment, and shear force. Both torsional and shear forces decrease progressively toward the midspan segment (ML12).
2) Prestress loss analysis across all tendon profiles shows that the greatest loss occurs in the bottom tendon profile, with a total loss of 272.22 MPa, equivalent to 19.94% of the initial prestressing stress.
3) Stress checks performed on each segment confirm that the box girder satisfies the allowable stress limits at both the immediate post-transfer stage and the service stage. At transfer, compressive and tensile stresses do not exceed 20.25 MPa and 1.25 MPa, respectively. Under service conditions, compressive and tensile stresses remain within 20.25 MPa and 3.35 MPa, respectively.
4) The deflection experienced by the box girder cross-section is within the allowable serviceability limits, with a maximum of 146.25 mm in the side span and 105.63 mm in the main span.
5) Structural capacity calculations yielded a flexural capacity of 1.20×10^6 kN.m at the support segment and 2.49×10^5 kN.m at the midspan segment. The torsional capacity is 3.36×10^4 kN.m at the support and 1.77×10^4 kN.m at the midspan. Shear capacities are 4.70×10^4 kN.m and 2.16 × 104 kN.m for the support and midspan segments, respectively.

References

1. H. Liu, J. Li, J. Zhang, and D. Pang, Decision analysis of a reinforcement scheme for in-service prestressed concrete box girder bridges based on ahp and evaluation of the reinforce(m)ent effect. Buildings MDPI, **12**(1771), 1–17 (2022). https://doi.org/10.3390/buildings12101771
2. M. Aghagholizadeh and N. Catbas, Comparative analysis and evaluation of two prestressed girder bridges. Current Trends in Civil & Structural Engineering, **3**(5), 1–9 (2019). https://doi.org/10.33552/ctcse.2019.03.000572
3. P. Agarwal and D. K. Singh, Parametric study on prestressed skewed box-girder bridge. Advances. In Bridge Engineereing. **4**(12), 3–26 (2023). https://doi.org/10.1186/s43251-023-00090-5
4. R. M. Arzanti, N. Rasidi, and Suhariyanto, *Perbandingan box girder dengan I-girder menggunakan metode balanced cantilever pada Jalan Tol Pandaan-Malang Sta. 35+380*. J. Management Rekayasa Konstruksi. **1**(3), 145–150 (2020) (in Indonesian). https://doi.org/10.55404/jos-mrk.2020.01.03.145-150
5. M. R. Trisnawardhana, B. Piscesa, and P. Suprobo, *Evaluasi perancangan Jembatan Longspan Cililitan proyek LRT Jabodebek menggunakan* balanced cantilever precast post-tensioned box girder. J. Teknologi ITS. **10**(1), C7–C13 (2021) (in Indonesian). https://doi.org/10.12962/j23373539.v10i1.59804
6. S. Ranje and B. J. Shah, Parametric study on analysis and design of precast segmental box girder type superstructure of bridge. Int. Adv. Res. J. Sci. Eng. Technol. **8(**4), 345–351 (2021). https://doi.org/10.17148/IARJSET.2021.8458
7. W. Kosim and F. Supartono, Analisis jembatan beton prategang box girder dengan metode balanced cantilever. Journal Mitra Teknik Sipil, **3**(2), 375 (2020). https://doi.org/10.24912/jmts.v3i2.6947
8. L. S. Kalaiselvan, Segmental analysis and design of superstructure for box girder balanced cantilever bridge by IRC specification using Midas Civil. International Journal of Advances Research in Science Communication and Technology, **8**(3), 107–114 (2020). https://doi.org/10.48175/ijarsct-305
9. T. Y. Lin and N. H. Burns, Desain struktur beton prategang. (1988).
10. E. G. Nawy, Reinforced concrete: A fundamental approach, 6th Edition (Prentice Hall, New Jersey, 2009)
11. F. Xu, Y. Cheng, K. Wang, and M. Zhou, Transverse analysis of box girders with corrugated steel webs. Buildings MDPI, **14**(3), 2–28 (2024). https://doi.org/10.3390/buildings14030574
12. J. Edmunds, L. Franco, T. Jayasinghe, T. Ginigaddara, P. Vaz-Serra, and P. Mendis, Bridge deck analysis of transversely post-tensioned concrete box girder bridges. Electronic Journal of Structural Engineering, **23**(1), 46–63 (2023). https://doi.org/10.56748/ejse.234101
13. Corven and John, Federal Highway Administration, Post-tensioned box girder design manual, (2016).
14. W.-F. Chen and L. Duan, Bridge Engineering Handbook, Superstructure design, 2nd Edition, (2012).
15. M. Rashed and S. S. F. Mehanny, Simulating creep induced moment redistribution in prestressed concrete bridges constructed by the balanced cantilever method: Ad hoc traditional formulae versus real time-dependent analysis. Journal Engineering. Applied Science. **70**(28), 1–23 (2023). https://doi.org/10.1186/s44147-023-00199-4